Influence of the filter in feedback loop on the operation of the nuclear magnetic resonance gyroscope

Zhao Hongchang[1], Zhan Xiang[1], Jiang Qiyuan[1], Wang Zhiguo[1,2*], Luo Hui[1,2]

(1. College of Advanced Interdisciplinary Studies, National University of Defense Technology, Changsha 410073, China;
2. Interdisciplinary Center of Quantum Information, National University of Defense Technology, Changsha 410073, China)

Abstract: In order to analyze the amplitude and frequency characteristics of the ^{129}Xe spin oscillator in the nuclear magnetic resonance gyroscope (NMRG), a corresponding theoretical model was established. The density matrix and the classical electromagnetic theory were utilized to describe the nuclear spin ensemble and the feedback system, respectively. An oscillation equation with self-consistency condition was obtained. Furthermore, the oscillation equation was simplified and expanded to self-consistency equations with rotating-wave and slow-varying approximations, which described the amplitude and frequency of the oscillator simultaneously. Based on the semiclassical model, the influence of a band-pass filter on the amplitude and frequency of the spin oscillator was investigated. The simulation results indicate that the typical frequency shift caused by unsuitable feedback loop may reach the magnitude of sub-micro Hz. Proposed model offers the potential to improve the performance of NMRG based on spin oscillators.

Key words: spin oscillator; nuclear magnetic resonance gyroscope; filter; self-consistency equations

CLC number: V241.5 **Document code:** A **DOI:** 10.3788/IRLA202049.0205008

核磁共振陀螺反馈环路中滤波器的影响研究

赵洪常[1],展 翔[1],江奇渊[1],汪之国[1,2*],罗 晖[1,2]

(1. 国防科技大学 前沿交叉学科学院,湖南 长沙 410073;
2. 国防科技大学 量子信息学科交叉中心,湖南 长沙 410073)

摘 要: 为了分析核磁共振陀螺中 ^{129}Xe 自旋振荡器的振幅和频率特性,建立了相应的半经典模型,其中分别采用密度矩阵和经典电磁理论描述核自旋系综和反馈系统。然后,根据自激振荡的自洽条件推导了用于描述自旋振荡器的振荡方程。进一步,利用旋转波近似和慢变振幅近似将振荡方程化简为自洽方程组,它由分别用于描述自旋振荡器振幅和频率的振幅方程和频率方程构成。基于上述自旋振荡器的半经典模型,研究了带通滤波器对自旋振荡器振幅和频率的影响。仿真结果表明,对核磁共振陀螺的典型参量,反馈环路设计不当导致的自旋振荡器频移可达亚 μHz。该研究对提高基于自旋振荡器的核磁共振陀螺性能具有一定的参考价值。

关键词: 自旋振荡器; 核磁共振陀螺; 滤波器; 自洽方程

收稿日期:2019-10-11; **修订日期:**2019-11-21

基金项目:国家自然科学基金(61671458);湖南省自然科学基金(2018JJ3608);国防科技大学校预研项目(ZK170204)

作者简介:赵洪常(1977-),男,副研究员,硕士,主要从事陀螺技术方面的研究。Email: hongchangzhao1977@163.com

通讯作者:汪之国(1982-),男,副教授,博士,主要从事陀螺技术方面的研究。Email: maxborn@nudt.edu.cn

0 Introduction

The nuclear magnetic resonance gyroscope (NMRG) has attracted much attention recently, since it has shown competitiveness to the mainstream gyros[1-10]. Its advantages include high precision, small size, resistance to shock and vibration, and so on. The NMRG measures rotation rates with frequency shift of the Larmor precession of spin ensembles in a constant magnetic field. Due to the relaxation effect within the spin ensembles, the duration of free precession is limited. Thus, a feedback loop is usually utilized to make the spin ensembles run as a spin oscillator[11-13]. Nevertheless, it may bring disadvantages since the spin oscillation frequency may be shifted by the feedback loop. The impact of the phase shift of the feedback loop, relaxation time, and operation mode[11-12] on oscillation frequency has been discussed for spin oscillators, while the impact of the filter within the feedback loop on oscillation frequency has not been reported, as far as we know.

In view of the ^{129}Xe spin oscillator, the density matrix and the classical electromagnetic theory are utilized to describe the nuclear spin ensembles and the feedback magnetic field, respectively. Then a semiclassical model of self-excited spin oscillator is founded utilizing self-consistency condition. Therefore, the impact of the filter within the feedback loop on oscillation frequency is discussed, which would give a guidance to improve the frequency stability of the NMRG.

1 Theory

The typical configuration of a ^{129}Xe nuclear spin oscillator is illustrated in Fig.1[1,12-13]. In the center of the setup, there is a spherical glass vapor cell filled with ^{129}Xe, ^{87}Rb, and buffer gases (N_2, etc.), which are utilized to provide the nuclear spin, electron spin, and quenching effect for the excited state rubidium atoms, respectively. We use the left-handed circularly polarized laser beam resonant with the D1 line of ^{87}Rb to optically pump the Rb atoms to its m_F=2 magnetic sublevel, thus making their spin polarized, and then making the ^{129}Xe nuclear spin hyper-polarized through spin-exchange between Rb-Xe to eventually form the longitudinal magnetic moment along Z axis.

The Z-coil produces static magnetic field along the Z axis, and the driving magnetic field along the X axis is generated by the X-coil to make the nuclear magnetic moment precess about the Z axis. In order to keep the nuclear magnetic

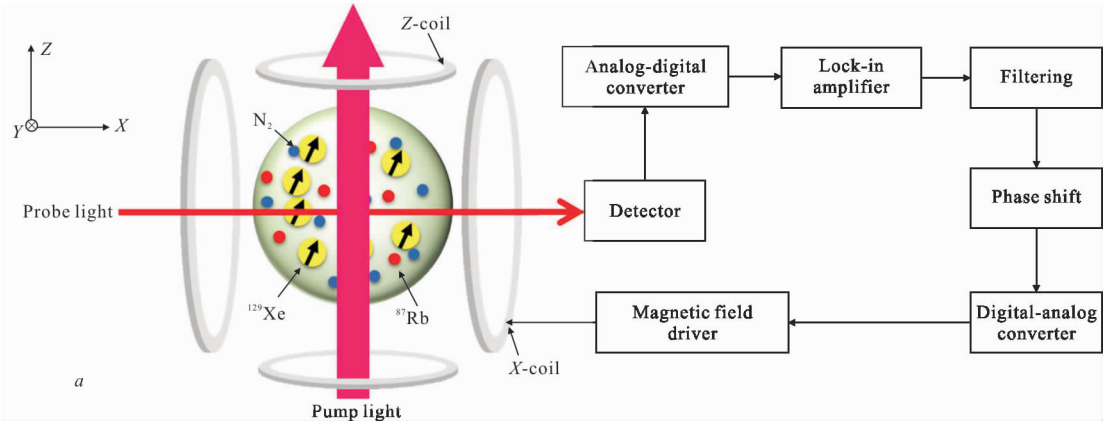

Fig.1 Configuration of the spin oscillator(Z-coil: The coil producing magnetic field along Z axis; X-coil: The coil producing magnetic field along X axis)

moment precessing continuously, we utilize electronic feedback system to constitute the feedback loop. The probe laser beam with linear polarization travels through the vapor cell along the *X* axis and impinges on the detector, whose output is digitalized via an analog –digital converter. Through the lock –in amplifier, the magnetic fields in the *X* and *Y* axes are sensed through the Rb magnetometer[1]. The *Y* component of the magnetic field produced by the nuclear spins is filtered, phase –shifted to generate the feedback signal. It is used to drive the *X* coils through the digital –analog converter and the magnetic field driver. In order to suppress noise and interference, a band–pass filter is usually used in the feedback loop, which could be described with the classical electromagnetic theory.

The quantum number of the ^{129}Xe nuclear spin is 1/2, therefore it would split into two magnetic sublevels within the magnetic field. We could treat its energy level structure as a simple two level model as illustrated in Fig.2. We assume that the energy difference between these two

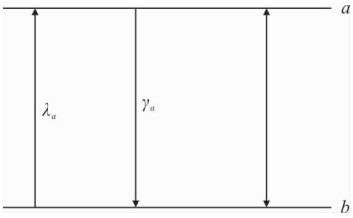

Fig.2 Two level model of the ^{129}Xe nuclear spin(λ_a: ρumping rate induced by polarized ^{87}Rb atoms; γ_a: relaxation rate caused by the collisions with the cell wall and buffer gases)

levels is $\hbar\omega_0$, and the pumping rate induced by polarized ^{87}Rb atoms is denoted as λ_a, meanwhile the relaxation rate caused by the collisions with the cell wall and buffer gases is γ_a. Here $\hbar$ is the Planck constant. Let the driving magnetic field along the *X* axis be $B_x=2B_1\cos(vt+\varphi)$, and the Hamiltonian of the system is[14]:

$$\hat{H}=\hat{H}_0+\hat{V}=-\hat{\mu}_z B_0-\hat{\mu}_x 2B_1\cos(vt+\varphi) \tag{1}$$

where $\hat{\mu}_z=\frac{1}{2}\gamma_g\hbar\begin{bmatrix}1&0\\0&-1\end{bmatrix}$, $\hat{\mu}_x=\frac{1}{2}\gamma_g\hbar\begin{bmatrix}0&1\\1&0\end{bmatrix}$, $2B_1$, v and φ are the amplitude, frequency and slow –varying phase of the driving field, respectively, t is time, γ_g is gyromagnetic ratio of the nuclear spin.

The state can be expressed as:

$$|\psi\rangle=c_a|a\rangle+c_b|b\rangle \tag{2}$$

where $|a\rangle$, $|b\rangle$ are the eigenstate, c_a, c_b are the probability amplitude of high and low energy level, respectively.

If we substitute Eq. (2) into Schrodinger equation $\frac{\mathrm{d}}{\mathrm{d}t}|\psi\rangle=\hat{H}|\psi\rangle$, c_a and c_b would satisfy the equations:

$$\begin{aligned}\dot{c}_a&=-ic_a\omega_0-\frac{i}{\hbar}c_b V_{ab}\\ \dot{c}_b&=-\frac{i}{\hbar}c_a V_{ba}\end{aligned} \tag{3}$$

where $V_{ab}=V_{ba}=-\gamma_g\hbar B_1\cos(vt+\varphi)$, and the "." on the head of the symbols denotes time derivative. For spin ensembles composed of substantial atoms, we could use density matrix to describe the state of spin, and the corresponding motion equations of matrix components according to Eq. (3) are as follows,

$$\dot{\rho}_{aa}=\lambda_a\rho_{bb}-\gamma_a\rho_{aa}-\left[\frac{i}{\hbar}V_{ab}\rho_{ba}+c.c.\right] \tag{4}$$

$$\dot{\rho}_{bb}=-\lambda_a\rho_{bb}+\gamma_a\rho_{aa}+\left[\frac{i}{\hbar}V_{ab}\rho_{ba}+c.c.\right] \tag{5}$$

$$\dot{\rho}_{ab}=-(i\omega_0+\gamma)\rho_{ab}+\frac{i}{\hbar}V_{ab}(\rho_{aa}-\rho_{bb}) \tag{6}$$

where γ denotes the decoherence rate, $\rho_{aa}=c_a c_a^*$, $\rho_{bb}=c_b c_b^*$, $\rho_{ab}=c_a c_b^*$, $\rho_{ba}=\rho_{ab}^*$. Due to the ^{129}Xe nuclear spin is an ideal two level model, we have $\rho_{aa}+\rho_{bb}=1$. The population probability difference between two levels is defined as:

$$w=\rho_{aa}-\rho_{bb}=2\rho_{aa}-1 \tag{7}$$

Eq. (7) could be used together with Eqs. (4) –

(6) to obtain the simplified motion equations:

$$\dot{w}=(\lambda_a-\gamma_a)-(\lambda_a+\gamma_a)w-2\left[\frac{i}{\hbar}V_{ab}\rho_{ba}+c.c.\right] \quad (8)$$

$$\dot{\rho}_{ab}=-(i\omega_0+\gamma)\rho_{ab}+\frac{i}{\hbar}V_{ab}w \quad (9)$$

Through comparing Eqs. (8) –(9) and the Bloch equation, we know $\gamma=1/T_2$ and $\lambda_a+\gamma_a=1/T_1$ for the spin ensemble[1, 14]. Here T_1 and T_2 are longitudinal and transverse relaxation time for spins in the NMRG, respectively.

In order to solve the motion equations above, we need to have a clear understanding of relationship between the feedback magnetic field B_x and the mean value of the transverse magnetic moment $\langle\mu_y\rangle$, and the latter could be expressed as:

$$\langle\mu_y\rangle=Tr(\mu_y\rho)=i\frac{1}{2}\gamma_g\hbar(\rho_{ab}-\rho_{ba}) \quad (10)$$

Let the signal before the band–pass filter be $m_y=-i\eta\ \langle\mu_y\rangle$, and the output of the filter is $\widetilde{B}_1$, where η is the transfer parameter of the system including magnetometer, photo–detector, analog–to–digital converter, and so on. They satisfy the following equation[15]:

$$\frac{\mathrm{d}^2}{\mathrm{d}t^2}\widetilde{B}_1+2\zeta\omega_n\frac{\mathrm{d}}{\mathrm{d}t}\widetilde{B}_1+\omega_n^2\widetilde{B}_1=2\zeta\omega_n^2 m_y \quad (11)$$

where ω_n and ζ are center frequency and damping factor of the filter, respectively.

Due to the similarity between the wave equation in electromagnetic theory and Eq. (11), we could regard the right side of Eq. (11) as the excitation source of the wave equation. When taking the phase shift of the electronic feedback system θ into account, the expression of m_y can be described as:

$$m_y=-i\eta\langle\mu_y\rangle=\frac{1}{2}\eta\gamma_g\hbar(\rho_{ab}\mathrm{e}^{-i\theta}-\rho_{ba}\mathrm{e}^{i\theta}) \quad (12)$$

2 Analytic solutions

Defining $\rho_{ab}=A\mathrm{e}^{-i(vt+\varphi)}$, $\widetilde{B}_1=B\mathrm{e}^{-i(vt+\varphi)}$, where A is real and B is complex. Under the rotating wave approximation and neglection of higher order terms, Eqs.(8) and (9) can be reduced to:

$$\dot{w}=(\lambda_a-\gamma_a)-(\lambda_a+\gamma_a)w+Re[i\gamma_a A^*B] \quad (13)$$

$$[\dot{A}-i(v+\dot{\varphi})A]=-(i\omega_0+\gamma)A-i\gamma_g wB \quad (14)$$

Substituting $\rho_{ab}=A\mathrm{e}^{-i(vt+\varphi)}$, $\widetilde{B}_1=B\mathrm{e}^{-i(vt+\varphi)}$ into Eq.(11), we have:

$$[-(v+\dot{\varphi})^2B]+2\zeta\omega_n[-i(v+\dot{\varphi})B]+\omega_n^2B=2\zeta\cdot\frac{1}{2}\eta\gamma_g\hbar[(v+\dot{\varphi})^2A]\mathrm{e}^{-i\theta} \quad (15)$$

from which the relation between A and B can be obtained by neglecting higher order terms,

$$B\approx\frac{1}{2}\eta\gamma_g\hbar\gamma_c\frac{(\omega_n-v)+i\gamma_c}{[(\omega_n-v)^2+\gamma_c^2]}A\mathrm{e}^{-i\theta}=T(v)A\mathrm{e}^{-i\theta} \quad (16)$$

where $\gamma_c=\zeta\omega_n$ denotes the bandwidth of the filter and $T(v)=\frac{1}{2}\eta\gamma_g\hbar\gamma_c\frac{(\omega_n-v)+i\gamma_c}{[(\omega_n-v)^2+\gamma_c^2]}$.

Eq. (16) gives the steady state relationship between A and B, which indicates that the impact of the band–pass filter could be expressed with the transfer function $T(v)$. By substituting Eq.(16) into Eq. (14) and extracting the imaginary part of the equation, the frequency equation could be obtained as:

$$v+\dot{\varphi}=\omega_0+\gamma\frac{(\omega_n-v)\cos\theta+\gamma_c\sin\theta}{\gamma_c\cos\theta-(\omega_n-v)\sin\theta} \quad (17)$$

When $\theta=0$, the oscillation frequency of the spin oscillator is:

$$v+\dot{\varphi}=\omega_0+\frac{\gamma}{\gamma_c}(\omega_n-v) \quad (18)$$

Eq. (18) indicates that under the condition of $\theta=0$, the actual frequency of the oscillator will shift from Larmor precession frequency and the amount of shift depends on detuning $\omega_n-\omega_0$ due to the band–pass filter. When the bandwidth of the band–pass filter is smaller or the coherence time of ^{129}Xe spin ensembles is shorter, the amount of frequency shift is larger. While $\omega_n=\omega_0$, the frequency shift is zero.

Furtherm ore, we could also extract the real part of Eq.(14) to obtain the following equation:

$$w=\frac{\gamma}{\gamma_g}\frac{1}{g_0}\frac{(\omega_n-v)^2+\gamma_c^2}{\gamma_c\cos\theta-(\omega_n-v)\sin\theta} \tag{19}$$

where $g_0=\frac{1}{2}\eta\gamma_g\hbar\gamma_c$. When $\theta=0$, we have $w=\frac{\gamma}{\gamma_g}$. $\frac{1}{g_0}\frac{(\omega_n-v)^2+\gamma_c^2}{\gamma_c}$, namely the band-pass filter could efficiently modify the feedback gain if the bandwidth is small.

If we substitute Eq.(19) into Eq.(13), we could obtain the expression of A,

$$A=\sqrt{\frac{1}{\gamma_g d}\left(w_0-\frac{\gamma\gamma_1}{\gamma_g d}\right)} \tag{20}$$

where $w_0=\lambda_a-\gamma_a$, $\frac{1}{d}=\frac{1}{g_0}\frac{(\omega_n-v)^2+\gamma_c^2}{\gamma_c\cos\theta-(\omega_n-v)\sin\theta}$, $\gamma_1=\lambda_a+\gamma_a$. The condition of continuously oscillation could be derived from Eq.(20) as:

$$w_0-\frac{\gamma\gamma_1}{\gamma_g d}>0 \tag{21}$$

Through rotating wave approximation, slow-varying amplitude and phase approximation, we obtained Eqs.(17) and (20). They are approximate solutions for frequency $v+\dot{\varphi}$ and amplitude m_y of the spin oscillator. In order to check them, we made numerical simulation based on Eqs.(8)-(11). With parameters $\gamma_g=2\pi\times10$ Hz, $\lambda_a+\gamma_a=1/T_1=0.033$ s^{-1}, $\lambda_a-\gamma_a=0.016$ s^{-1}, $\gamma=1/T_2=0.05$ s^{-1}, $\eta\gamma_g\hbar=0.01$ μT, $\theta=0$, we obtained $v+\dot{\varphi}$ and m_y as a function of detuning $(\omega_n-\omega_0)/(2\pi)$ at different bandwidth $\Delta f=\gamma_c/(2\pi)$. Meanwhile, approximate solutions of oscillation frequency and amplitude of the spin oscillator are also given, based on Eqs.(18) and (20). The resu lts are shown in Fig.3 and Fig.4 respectively, where "num." in the legend represents solutions from numerical simulation and "appr." represents solutions from approximate Eqs. (18) and (20).

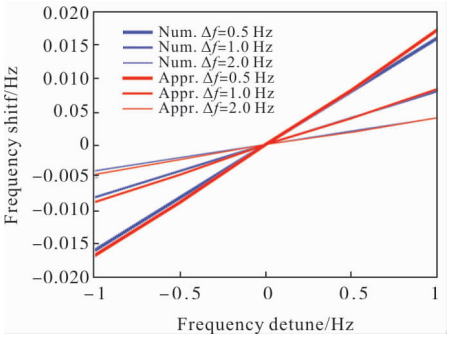

(a) B_0=2 μT

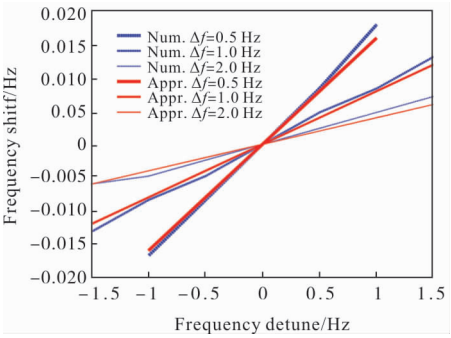

(b) B_0=10 μT

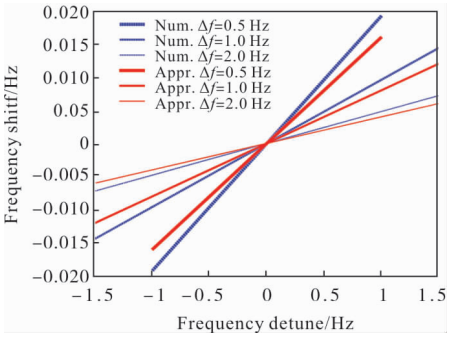

(c) B_0=20 μT

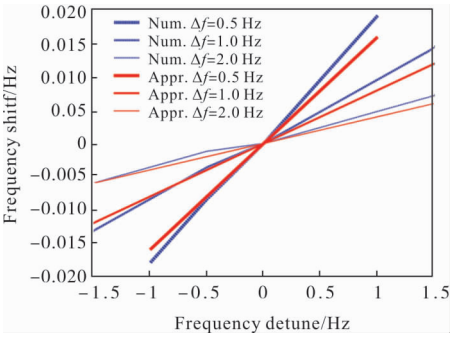

(d) B_0=50 μT

Fig.3 Oscillation frequency shifts of the spin oscillator vs frequency detuning at different bandwidth of band-pass filter

It is clear that approximate solutions agree well with numerical simulation in all of the

figures. According to Eq. (18), we have $v=\left(\omega_0+\frac{\gamma}{\gamma_c}\omega_n\right)/\left(1+\frac{\gamma}{\gamma_c}\right)$. Since $\frac{\gamma}{\gamma_c}<<1$ is true for a typical spin oscillator, the oscillation frequency is mainly determined by Larmor frequency of the spins. The band-pass filter leads to a small frequency shift towards the center frequency, and the narrower the filter bandwidth, the larger the frequency shift. As for the amplitude of the spin oscillator, it is surprising that the amplitude as a function of frequency detuning has a valley in the center of the filter. Through careful checking, we found A^2 in Eq.(20) is a quadratic function of $1/d$, which depends on ω_n-v. The peak of the quadratic function is not located at $\omega_n=\omega_0$. According to the Figs.(3) and (4), we found the narrower the filter bandwidth, the larger the errors of the approximate solution. The reason is that there are several approximations in the derivation. When $\theta\neq 0$ the frequency and amplitude of the spin oscillator can also be obtained from Eqs.(17) and (20).

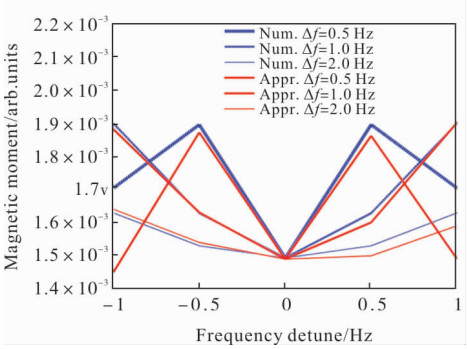

(a) B_0=2 μT

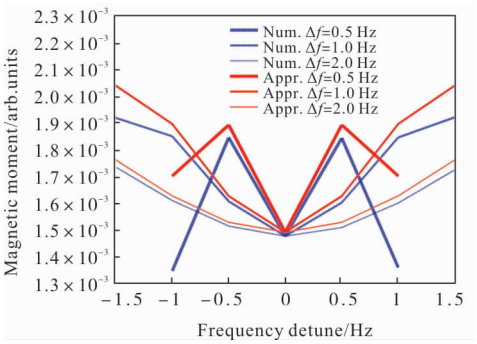

(b) B_0=10 μT

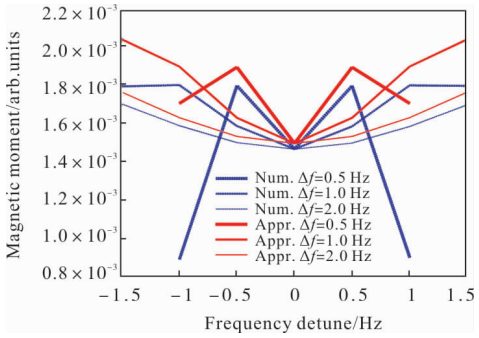

(c) B_0=20 μT

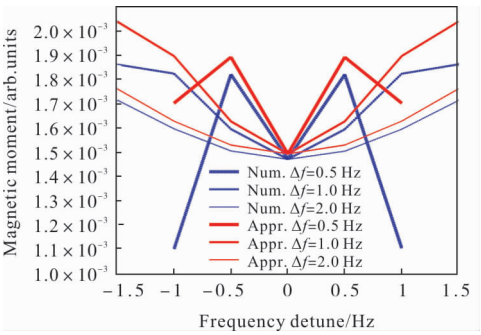

(d) B_0=50 μT

Fig.4 Precessing magnetic moment vs. frequency detuning at different bandwidth of band-pass filter

3 Discussions

3.1 Comparison with semiclassical laser physics theory

Plenty of coincidence could be found between the semiclassical theory of spin oscillator and the laser physics[14], while differences would also give guidance to our analysis. According to the semiclassical theory of laser physics, generally the bandwidth of the laser resonant cavity is far smaller than that of the gain medium, thus, the actual lasing frequency is mainly determined by the resonant frequency of the cavity, while the frequency pulling and pushing effect of the gain medium could only modify slightly the laser frequency to the magnitude of 10^{-3}. Nevertheless, for the case of the spin oscillator, the linewidth of the spin ensembles is much smaller than that of the filter, which makes the oscillation frequency mainly determined by the Larmor frequency of

the spin ensembles, and only slight modification on the oscillation frequency could be obtained from the filter.

3.2 Impact of the filter in the feedback loop

In order to make the oscillator working continuously, a feedback loop must be applied, which would inevitably influence its frequency due to the amplitude –frequency and phase – frequency characteristics of the filter. With typical parameters of the ^{129}Xe spin oscillator as γ=0.05 s^{-1}, γ_c=10 Hz, $(\omega_n-\omega_0)/(2\pi)$=1 Hz, the amount of induced frequency shift effect is 0.005 Hz. Under certain conditions, decoherence rate γ is approximately proportional to the density of ^{87}Rb[12], which varies severely with temperature. We may use the formula of the density of ^{87}Rb as a function of temperature in [16] to estimate the frequency shift change with the temperature fluctuation. A temperature variation of 0.001 ℃ will make the ^{87}Rb density vary relatively 10^{-4}, which leads to the estimated frequency pulling of 0.5 μHz. This is already a severe error for high precision measurement. This error can be reduced through careful design of the filter in the feedback loop.

The filter also decreases the scale factor of the spin oscillator for measuring rotation or other physical effect. According to Eq. (18), the scale factor of the spin oscillator is $1/(1+\gamma/\gamma_c)$. If the filter has so narrow a bandwidth that γ/γ_c>0.1, a sensitivity reduction would occur. This will lead to a failure for the NMRG as a primary rotation sensor[17].

4 Conclusions

In this paper, the semiclassical model of the ^{129}Xe nuclear spin oscillator was established, which further leads to the approximately obtained equations of amplitude and frequency. Both approximately analytic solution and numerical solution indicated that the frequency of the spin oscillator is mainly determined by the Larmor precession frequency of spin ensembles, and the filter in the feedback system would cause the oscillation frequency shift effect. It showed that the narrower the filter bandwidth, the larger the frequency shift effect in a typical NMRG system. So the filter in the NMRGs should be designed carefully.

References:

[1] Eklund E J. Micro gyroscope based on spin–polarized Nuclei [D]. California: University of California at Irvine, 2008.

[2] Larsen M, Bulatowicz M. Nuclear magnetic resonance gyroscope [C]// IEEE Frequency Control Symposium Proceeding, 2012: 1–5.

[3] Donley E. Nuclear magnetic resonance gyroscopes [C]// Proceedings of the Sensors, 2010 IEEE, 2010: 17–22.

[4] Fang Jiancheng, Qin Jie. Advances in atomic gyroscopes: A view from inertial navigation applications[J]. ***Sensors***, 2012, 12(5): 6331–6346.

[5] Qin Jie, Wang Shilin, Gao Puze, et al. Advances in nuclear magnetic resonance gyroscope [J]. ***Navigation Positioning & Timing***, 2014, 1(2): 64–69. (in Chinese)

[6] Wan Shuang′ai, Sun Xiaoguang, Zheng Xin, et al. Prospective development of nuclear magnetic resonance gyroscope [J]. ***Navigation Positioning & Timing***, 2017, 4(1): 7–13. (in Chinese)

[7] Zhou Binquan, Lei Guanqun, Chen Linlin, et al. Noise suppression for the detection laser of a nuclear magnetic resonance gyroscope based on a liquid crystal variable retarder [J]. ***Chinese Optics Letters***, 2017, 15 (8): 99–103.

[8] Liu Yuanxing, Wang Wei, Wang Xuefeng. Key technology and development tendency of micro nuclear magnetic resonance gyroscope [J]. ***Navigation and Control***, 2014, 13(4): 1–6. (in Chinese)

[9] Li Pan, Liu Yuanzheng, Wang Jiliang. Current status and development of nuclear magnetic resonance microgyroscopes [J]. ***Micronanoelectronic Technology***, 2012, 49(12): 769–774, 785. (in Chinese)

[10] Yi Xin, Wang Zhiguo, Xia Tao, et al. Research on temperature field in the vapor cell of nuclear magnetic

resonance gyroscope [J]. ***Chinese Optics***, 2016, 9(6): 671−677. (in Chinese)

[11] Wang Zhiguo, Peng Xiang, Luo Hui, et al. Comparison of operation modes for spin −exchange optically − pumped spin oscillators [J]. ***Journal of Magnetic Resonance***, 2017, 278: 134−140.

[12] Walker T G, Larsen M S. Spin−exchange pumped NMR gyros [J]. ***Advances in Atomic, Molecular, and Optical Physics***, 2016, 65: 373−401.

[13] Yoshimi A, Inoue T, Furukawa T, et al. Low−frequency ^{129}Xe nuclear spin oscillator with optical spin detection [J]. ***Physics Letters A***, 2012, 376: 1924−1929.

[14] Sargent M, Scully M O, Lamb W E. Laser Physics[M]. New York: Addison−Wesley Publishing Company, 1974.

[15] Oppenheim V A, Willsky S A. Signals and Systems[M]. New Jersey: Prentice−Hall, 2017.

[16] Xu Guowei, Zhang Yi, Jiang Qiyuan, et al. Temperature control of vapor cell based on the light absorption of nuclear magnetic resonance gyroscope [J]. ***Infrared and Laser Engineering***, 2019, 48(S1): S106003. (in Chinese)

[17] Bevan D, Bulatowicz M, Clark P, et al. Nuclear magnetic resonance gyroscope: developing a primary rotation sensor[C]//2018 IEEE International Symposium on Inertial Sensors and Systems, 2018.